Antarctic Research, Vol. 2, No. 2, 24~37, December 1991

CHARACTERISTICS OF THE ACTIVE LAYERS ON FILDES PENINSULA OF KING GEORGE ISLAND, ANTARCTICA

Zhu Cheng[1], Cui Zhijiu[2] and Xiong Hei-gang[3]

[1] *Department of Geography, East China Normal University*
[2] *Department of Geography, Peking University*
[3] *Department of Geography, Xinjiang University*

Abstract From the data of the pitting, geoelectrical prospecting, temperature measurement, salt content analysis and detection by layering frost-heaving instruments, the authors discuss firstly the structural features of sediments in the active layers in this region, and proves the presence of the bowl-shaped frost table in the stone-circles area, and then analyse the regulatities of temperature distribution in the active layer, effect of salt content on electric resistivity, thaw-settlement and frost-heaving, and their control on periglacial land-form development. It suggests that the five layers should exist in the subsurface structure , namely, active layer, frost sand and gravel layer, frost volcanic rock permeated by sea water, frost volcanic rock unpermeated by sea water, and unfrost ancient continental basement. Finally, the permafrost table and its vertical gradient are deduced.
Key words Active layer, Permafrost table, Bowl-shaped frost table, Salt content, Geoelectrical Prospecting

Fildes Peninsula, 10 km long, 2.5—4 km wide and about 30 km^2 in area, is located in the ice-free area on the south end of King George Island of the South Sheltland Islands. According to the meteorological data obtained from 1985 to 1988 at the Great Wall Station, the annual mean air temperature is —3.3°C, and the annual mean precipitation is 605 mm. Before our station was set up, some foreign scientists had investigated the geology and geomorphology of the area (John, 1972; Araya & Herve, 1972). Since the establishment of our station in 1985, Zhang Qinsong and Xie Youyu and others have investigated and mapped the features of glacial-periglacial landform and the chemical weathering. Liu Xiaohan & Zhen Xiangshen have investigated the volcanic rocks in the area. Considering that the temperature and the frost-thawing status of active layer (i.e. the surface layer melting in summer and freezing in winter) is an important factor affecting on the periglacial landform development, we have carried out the pitting, measurements, geoelectrical prospecting, geotemperature analysis for studying the characteristics of the surface active layer in the area. The results are described in following sections.

1. Structural features of the sediments

Topographically the Fildes Peninsula are mostly composed of hills, beaches and swamps, the elevation of the highest peak, Huoshangjing, is 164.2 m a.s. l. On of the top of hills the volcanic rocks are exposed. The Quaternary sediments are usually very thin. In order to understand the features of the active layer, first of all, we carried out eight pittings. Their positions are showed in Fig. 1. The pit "G" is located on the top of Youyi Peak (99 m a. s. l.).

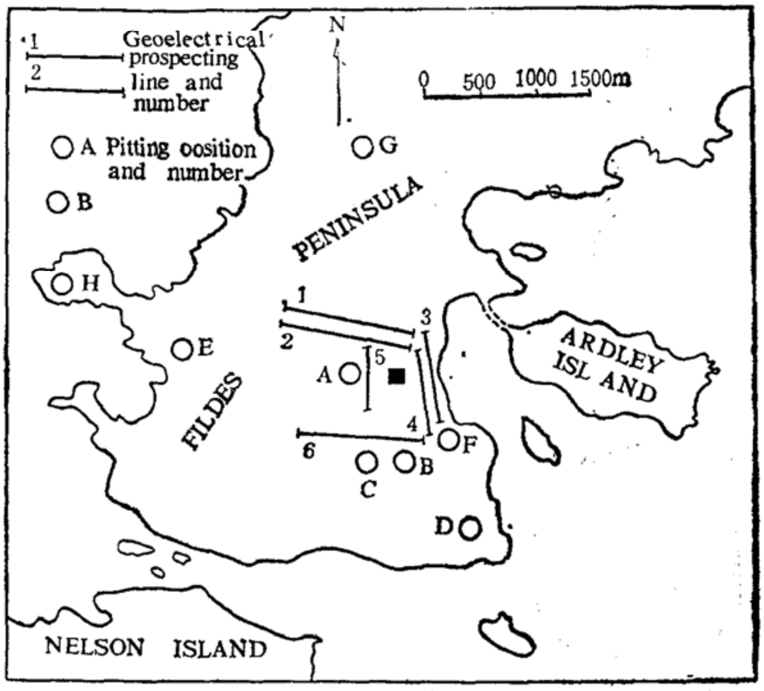

Fig. 1. Location of the pittings and sites of geoelectrical prospecting.

The sediments on the top are mainly volcanic clastic materials after frost riving of paleomarine-erosion stack and niche. They are only 30 —40 cm thick. On the half way up to the hill, the sediments are only half meter thick or so. We didn't find the frozen feature of the surface sediments except the frozen bedrock at the deep place. Pit "H" is situated on the northern cape of the western Biology Gulf on the peninsula. Here the biomass accumulation is 10—50 cm thick, it consists of a large number of shells which remained after sea-birds' eating. A pitting investigation in February of 1989 shows that the structure of the shell layer is loose and unfrozen.

Pit "A" is on the slope of the Astrofix Hill at elevation of 24.2 m a.s. l. in the Great Wall Station area. The profile of pit "A" exhibits six different layers (Fig. 2). Although the frozen ground with granular ice can be found at 0.42 m depth, and continues down to 1.5 m depth where a large number of ice lenses and massive ice are found after our dig and sampling analysis. The maximumcontent of water is 136.42% on the profile, it is just the characteristic of the permafrost table. Though the active layer is thicker, and grain size is smaller, no evidence of periglacial lendform (such as stone circles or striated soil, etc) was found. That is because of sea-water action and high salt content (see following discussion).

Pits "B" and "C" are located on the top of southern hill (41 m a. s. l.) near Yanou Lake. Here the sorted debris-type circles consist of angular or subangular volcanic debris. Two sorted debris-type circles were digged down to 1.3 m depth on January 28th and 29th of 1989 respectively. The profile of pit "B" is shown in Fig. 3. This sorted circle has a long axis of 2.8 m, and short axis of 2.5 m. Fig.3 shows that the grain-size distribution and the water (ice) content are different between the center and the edge of the stone circle. On the edge of the stone circle, the grain size of debris is coarser, and its maximum water content (210%) is found at 50—60 cm depth from the surface. At the center of the stone circle, the grain size is smaller and its maximum water content is found at 60—70 cm. It indicates that the permafrost table on the edge is about 10 cm

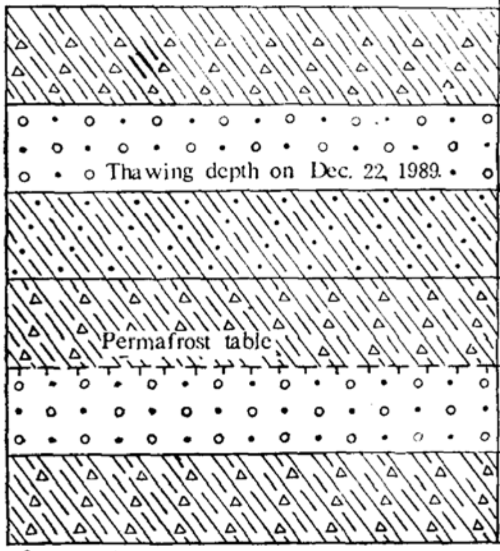

Layer order	Depth (m)	Profile feature	Pema-frost struc-ture	water content (%)	Tempera-ture (℃)
1	0 • 0.13	Brown soil with gravel, gravel 21. 85% sand 39.95% Silt-clay 38%, loose texture	Thawing Thawing	14.76	0.4～0.5
2	0.13-0.42	Brown fine-debris soil with gravel 15.48%, sand 33.51%, silt-clay 51.02%		12.49	0.4～-0.2
3	0.42-0.91	Brown sandy-clay, sand 40.71% sand-silt 38.74%, clay 14.25%, hard terture	Frozen ground with particle ice	34.76	-0.2～-0.4
4	0.91-1.50	Brown soil with gravel 20.84%, sand 37.01% silt-clay 43%, hard texture		94.87	-0.4～-1.3
5	1.50-1.64	Brown fine-debris soil, gravel 17.4%, sand 44.8%, silt-clay 38%, hard text.	*	136.42	-1.3～-2.2
6	1.64-2.60	Brown soil with gravel 22%, sand 44%, silt-clay 34%, hard texture	* *	83.12	-2.2～-2.3

* large number of ice lenses, massive ice; * * with ice lenses and massive ice

Note: Grain size and water content are from results of indoor analyses

Fig. 2. Profile of the pit No. A on Astrofix Hill.

shallower than that at the center. It can be seen on the whole profile that the shape of the permafrost table is concave at the center (Fig. 4).

We attribute the formation of the bowl-shaped permafrost table to the following factors.

1. The depth range of the marginal debris is only 40 cm or so, but the geotemperature is minus value here at the end of the hottest January. The shallower marginal debris layer, therefore, only plays a role in percolation of snow-melt water down to lower frost table to freeze it, while the heat conductivity of the debris only plays a minor role in the area. Its permeability is of first importance to promote freezing lower layer.

2. The high density of the central fine grained part, which hinders water from removing to frost table, is just a main cause for less ice -content at upper layer and deeper permafrost table at the center.

3. That the margin has more permeable water than other parts leads to its higher ice content, longer freezing time and stronger freezing intensity than at the center.

The three factors above are the main reasons for formation of bowl-shaped frost table at the sorted circle in the region.

Striated soil (see p 86 Photo 1) is a kind of periglacial landform which is most widely distributed in the active layer on Fildes Peninsula, and remains on the wide slope range. Our measurement indicates that the striated soil can be developed on the slope at angle $>3°$, and about 35° in maximum. Our naked eyes could see a liquidoid-flowing feature of the fine-grained part. When one walks through a striated soil area with higher water content, usually his feet may slightly sink into it. We digged some striated soil profiles at Half Triangle (Fig 1, pit "D"), second terrace of the western coast (Fig 1, pit "E"), the site near Geomagnetic Station and the site near the King Sejong Station on Barton Peninsula (Fig. 5). Meanwhile, we also analysed the water content and grain size of each layer. Pitting and indoor analysis show that the striated-soil can be divided into 5 parts: 1. surface coarse gravels (93.11 %has

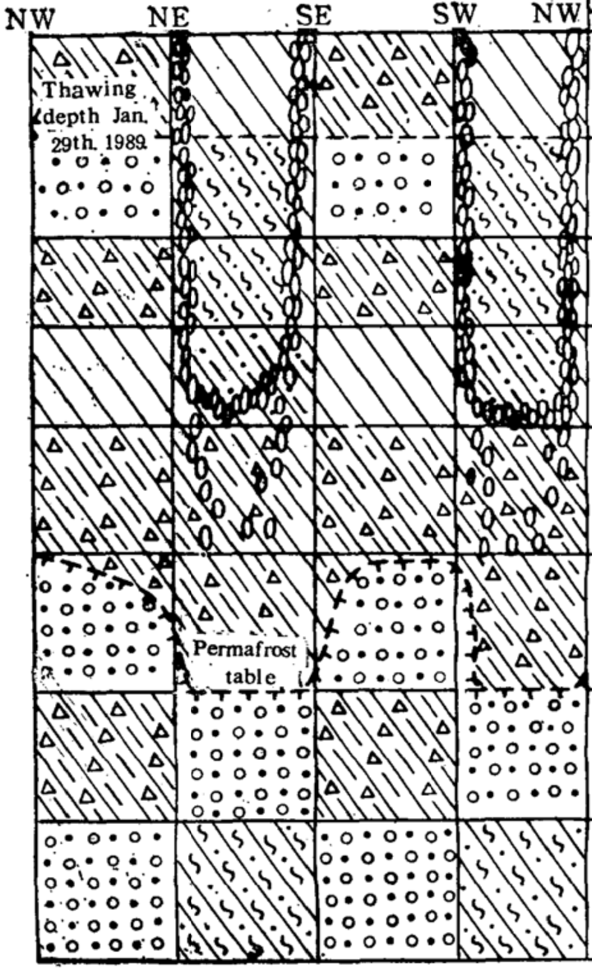

Layer order	Depth (cm)	Feature of stone circle profile: Center	Feature of stone circle profile: Edge	Permafrost structure: Center	Permafrost structure: Edge	Tem. (℃)	Water content (%): Center	Water content (%): Edge
1	5		Brown Soil with gravel 32%, sand 47%, silt-clay 20%, loose texture	Thawing	Thawing	0.2		14.9
2	10 ~ 20	Brown sand soil, sand 50%, Silt 41%, clay 6.7%, tight text.	Brown fine-debris Soil with gravel 18%, sand 45%, silt 36%	Frozen ground withice (thick2-4mm)	Frozen ground with ice debris	−0.2	89.09	166.4
3	20 ~ 30		Brown soil with gravel 38%, sand 55%, silt-clay 7%, hard tex			−1.1		149.2
4	30 ~ 40	Brown sand soil sand 55%, silt 25.7%, clay 9.3%, hard texture		Frozen ground with ice lenses	Frozen ground with ice debris	−1.8	21.35	
5	40 ~ 50	Brown soil with gravel 31.5% sand 51.34% silt clay 16%, hardtex	Deeper-grey soil with gravel 33.62%, sand 57.7%, silt clay 7%, hard texture		Frozen ground with ice lenses	−2.1	17.01	116.4
6	50 ~ 60	Deeper-grey soil with gra-vel 25.84%, sand 49.76% silt-clay 23.99%, hard text.	Deeper-grey soil with gravel 16.02% sand 63.75% silt clay 20.01%			−2.4	36.51	210
7	60 ~ 70	Deeper-grey fine debris soil with gravel 19.01%, sand 46.8%, silt clay 33.99%, hard text	Deeper-grey soil with gravel 22.2%, sand 60.75%, silt-clay 17%, hard texture			−2.5	185	53.75
8	70 ~ 130	Deeper-grey sandy clay, sand 59.56%, silt 24.05%, clay 7.98%, hard text	Deeper-grey fine debris soil with% gravel 15.54% sand 75.11%, silt 9% hard text.			−2.6	166	42.31

Note: Grain size and water content are from results of indoor analyses

Fig. 3. Profile of pit No. B across a sorted-debris circle.

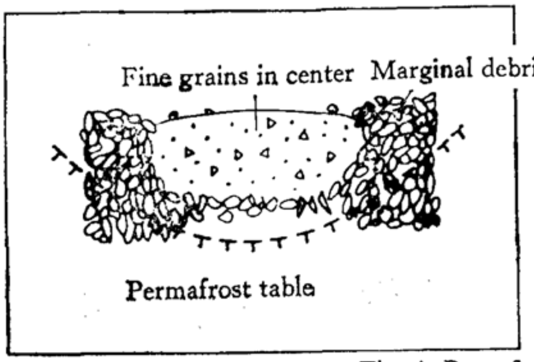

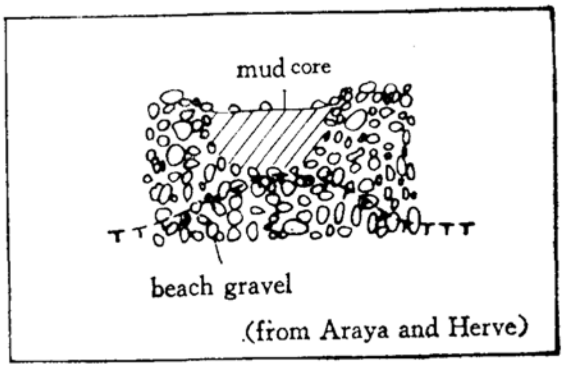

Fig. 4. Permafrost table at the sorted-debris circle.

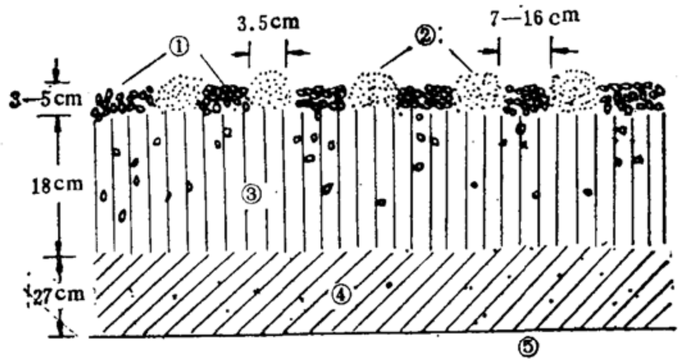

Fig. 5. Structural profile of the striated soil. ①debris, ②fine-debris with gravel, ③sandy soil, ④soil with debris, ⑤parmafrost with debris.

grain size of > 2 mm and 6.18%of 2—0.05mm); 2. surface fine debris soil (14.39% of >2 mm, 55.31% of 2—0.05 mm, 30.01% of <0.05mm) with gravels; 3. central sand-soil layer (81.84% of 2-0.05mm, 10.12% of 0.05—0.005 mm); 4. lower soil layer with gravels (33.21% of >2mm, 40.62% of 2—0.05mm, 25.99% of < 0.05mm); 5. permafrost layer with gravels (is the same as found in stone circle area). Our analysis indicates that the water content is low, only 8—16% in the surface fine-debris soil with gravels, 18—20% in central sand soil, and above 20% in lower soil layer with gravels.

Striated soil has its creep-flowing feature. The observation on the ground deformation with 4 surveying rods (thin steel bar of 0.5 m long) set in the place between Flat Mt. and Geomagnetic Station from January 14th to February 19th of 1989, indicates that all the rods moved down slope, with their velocity 45 cm in maximum, 3 cm in minimum, and 14 cm in average. If only 3 months in summer is counted(excluding winter since it is frozen or snowy), their seasonal creep-movement is 42 mm. The rate is also surprising. Another periglacial landform is debris flower which is a rare landforms in china. Photo 2(see p86) shows the debris flower, which is widely distributed on the southern highland near Yan'ou Lake in the area. The debris is 5.8 m long, 2 m wide, with its sedimentary surface dipping to 175° SE at a slope angle of 20°. Its lithology is flaly basaltic clastics with pores and amygdaloidal structure. We measured fabric of 100 fragments from the debris flower arranged in different directions. The result is shown in Fig. 6.

It can be seen in Fig. 6 and analysis of the measurement data that the dip of AB plane is not certainly related with slope orientation of the sedimentary surface. The AB plane extends evenly. However, the main dense part, to which the AB plane dips, still has a maximal value (47%) at 275°

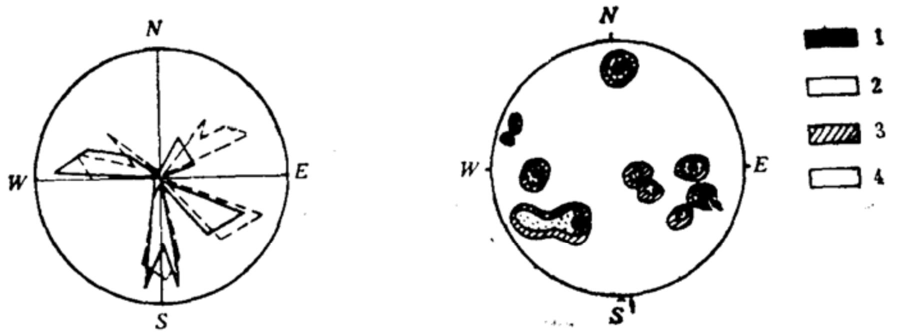

Fig. 6. Debris fabric (right) and rose diagram (left) of AB plane of the debris flower. right: Dotted line shows orientation, solid line shows left: main density, 1. >23%; 2. 15—23%, 3. 7—15%; 4. 4.0—7%; "↓" shows slope direction of the sedimentary surface.

SW, indicating an angle of about 100° between the dominative dip and slope orientation of the sedimentary surface. The specific debris fabric formed by frost thawing-sorting in active layer is very rare in China, since the self-adjustment-arrangment pattern of the debris formed by frost thawing-sorting is different from rock glacier (Zhu Cheng, 1989), talus (Zhu Cheng & Cui Zhi-jiu, 1988), till and debris flow (Shi Yafeng *et al.*, 1989). If we can precisely observe its internal adjustment and micro-change, we will deeper understand the real process of frost-thawing in the active layer.

2. Effect of temperature and water content on thawing-settlement and frost-heaving of active layer in summer

In order to observe the distribution of annual temperature in active layer, we installed IMD-85A automatic data-collecting instrument on December 25, 1987 on the top (30 m a.s. l.) of Badaling Hill at 100 m from the Great Wall Station. The instrument was made by Lanzhou Institute of Glaciology and Cryopedology. The observation objects are the followings:

1. Geotemperature and air temperature

We used integrated temperature sensor AD 590 to observe the temperature. The temperature-measuring range of the instrument is —55°C —+85°C. The geotemperature is measured by three groups of thermocouples (each group of 4 probes) which are separately buried at different underground depths. The air temperature and ground-surface temperature are measured by another group of thermocouple (also 4 probes).

2. Frost-heaving and displacement

First of all, we used variable resistor as temperature-transfer element. Two groups of sensors were used, two sensors of each group were installed at different underground depths to measure the frost-heaving and removing process. The instrument has a "CMOS" micro-computer system and a computer RAM with capacity of 10 K Byte. It is supplied with battery power and can automatically observe and record.

Fig. 7 shows a temperature curve obtained from the surface (at 30 m a.s.l.) down to 100cm depth on the top of Badaling Peak by instruments in 1988. We can see in Fig. 7:

1. The temperature curve fluctuates considerably on the ground surface and at underground 40 cm, but is smooth at 100 cm depth. It reflects a great temperature change on the ground sur-

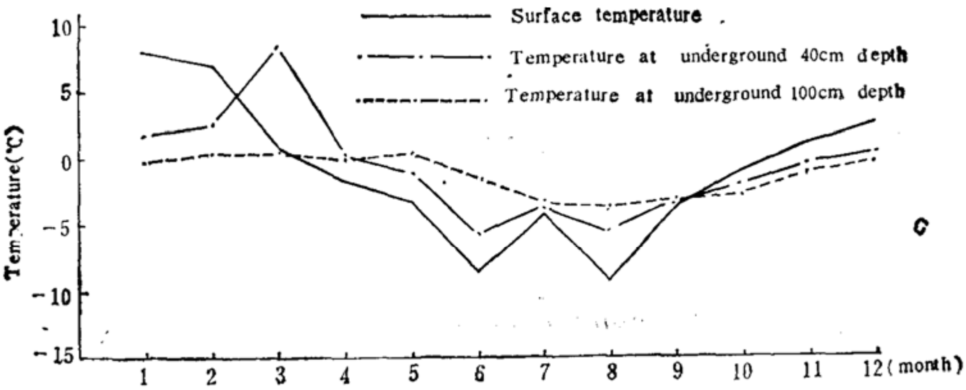

Fig. 7. Temperature curve from surface to underground 100 cm at Badaling Hill (30 m a. s. l.), Great wall Station, 1988.

face and in the upper ground layer and a great monthly temperature difference, but a small change and difference in the lower layer at 100 cm depth.

2. The maximum temperature appears on the ground surface in January (7.86°C), and at 40 cm depth in March (8.17°C), but at 100 cm depth in May (0.2°C). It shows that the temperature change obviously delays from the ground surface down to depth . So does the minimum temperature. For example, the mimimum temperature, appears on ground surface twice (in June and August respectively), at 40 cm depth in June (−5.8°C), and at 100cm depth in August (−3.65°C)

3. The temperature at 100 cm depth remains minus for 8 months of a year, but the temperature of each layer is plus from February to March.

From the geotemperature data of all layers, we calculated the depth of permafrost table to be 1.05 m at the site (30 m a.s. l.) where the data were collected.

The effect of temperature and water content on the frost-thawing of active layer sediments is also revealed by the experiments of artificial watering into three sorted debris circles for observing their changes on the southern highland (41 m a. s. l.) near Yan'ou Lake from January 13th to February 16th of 1989. Among the circles, the circle No. 1 has its long axis of 1.4 m, No. 2 of 1.7 m and No. 3. of 2 m diameter (see P.86 Photo 3).

The watering was conducted on January 16th and February 7th respectively. We used Swiss DI-20 infrared distance gauge and WILD-T_2 precise theodolite (with angular precision of ± 1.8″, and distance precision of 3 ^{mm}+1 ^{ppm}) to survey repeatedly by a fixed-point intersection method before and after watering. For the first watering (fresh water from Yan'ou Lake, with temperature of 5°C, air temperature 4°C, ground surface temperature 5°C, and temperature at 20 cm depth is 0.3°C), the circle No. 1 is watered 100 liters, and No. 2 50 litres, but, for a comparison, No. 3 is not watered. A survey conducted 5 days later after watering, indicates that the circle No. 1 with maximum water content has a mean displacement of 5.7 cm at its outer edge, with its general tendency being a contraction of 0.38 cm from outer to centre. In comparison the central 5 surveying rods has an average displacement of 3.1 cm, and general tendency is a contraction of 0.5 cm from outer to centre. Unwatered circle No. 3 has only an average displacement of 1.32 cm at its outer edge, and its general tendency is also contraction (average displacement of 0.32 cm). The displacement value of circle No. 2 is that between circles No. 1 and No. 3. Meanwhile, the surveying results, indicate that on either the watered stone circle or the unwatered circle, the surveying rods have settled from Jan. 13 to 22 (after the first watering). Surveying points on the outer edge have an average settlement value of 2.3 and 5. 5 cm at the center of circle. According to corelation coefficient:

$$r=\frac{S_{xy}}{S_x \cdot S_y}=\frac{\sum_{i=1}^{N}(x_i-\bar{x})\cdot(y_i-\bar{y})}{\sqrt{\sum_{i=1}^{N}(x_i-\bar{x})^2\cdot\sum_{i=1}^{N}(y_i-\bar{y})^2}} \quad (-1<r<1)$$

The statistics of data indicates that the displacement value of surveying points on the stone circle, to a certain degree, is correlated to geotemperature and watering amount. The correlation coefficient to the former is 0.65, and to the later is 0.61. The fact suggests that the thawing of the active layer and displacement and settlement of surface material are the general tendency for development of stone circle (artificial watering only accelerate the thawing and settlement) in January and February when the air temperature and ground temperature reach their highest peak. In general, the thawing and settlement in summer is an inexorable law. In addition, the sattlement of central part is 3.2 cm faster than the outer edge of stone circle. The frost-heaving features of the sediments in active layer are determined from the data obtained by the layering frost-heaving instrument installed on January 11th of 1989 after pitting on the Astrofix Hill top and on the stone circle of southern highland near Yan'ou Lake (see p86 photo 4). On the Astrofix Hill top, totally 10 layering frostheaving tubes were installed at the different depths. 0.3, 0.5, 0.7, 0.9, 1.1, 1.3, 1.5, 1.7, 1.8 and 1.875 m respectively). The surveying reference marks are alloy rods anchored at the 2.2 m depth in permafrost layer. The change of the layering frost-heaving tubes were measured 4 times in one year after their installation (Table 1 A). An interesting phenomenon is revealed from our measurement results, that is, the surveying rods at depth less than 1.3 m show a general tendency to settlement. A maximum settlement (1.1 cm) was found at 0.5 m depth. The average settlement value is 0.8 cm for the 5 tubes, but the other 5 tubes at 1.3—1.875m depth show an up lifting phenomenon. The maximum up lifting (0.9cm) takes place at 1.7 m depth, with an average up lifting value of 0.6 cm for the 5 tubes.

On the southern highland near Yan'ou Lake, the stone circle also shows a phenomenon of "settlement of Upper part and up lifting of lower part". 4 repeated surveys on all the 5 frost-heaving tubes (at 0.3, 0.7, 0.9, 1.1 and 1.3 m depths respectively) indicate that three tubes installed at above 0.9m depth show up lifting and another two show settlement. The mean settlement value is 2 mm, and up lifting is 1.4 cm (Table 1B). We consider that the difference of the frost-heaving-thaw-settlement is related to the salt content in the active layer in the area (discussed latter).

3. Electrical resistivity and salt content in active layer

In order to understand the electrical property, thickness and frost state of the active layer, we carried out the geoelectrical prospecting. Fig. 1 shows the sites for prospecting.

First of all, we tested the electrical parameter of a part of geological bodies on the peninsula (Zhen Xiang shen helped us drill and arrange electrodes on volcanic rock), so that we could infer deep lithology from the electrical resistivities. Table 2 shows the result.

Our investigation revealed that the lithology in the area are mainly of volcanic agglomerate, basalt and volcanic breccia. These bed rocks have high porosity and air-bubble, as well as amygdaloidal structure. The electrical resistivities of the exposed bed rock are 300–800Ωm, but it decreases down to 2.2–4.9 Ω m after irrigating with sea water. It is worth notice that a

Table 1. Change values of active lager frost-heaving in struments

(A)

Depth (m)	0.3	Diffe-rence(cm)	0.5	Diffe-rence(cm)	0.7	Diffe-rence(cm)	0.9	Diffe-rence(cm)	1.1	Diffe-rence(cm)	1.3	Diffe-rence(cm)	1.5	Diffe-rence(cm)	1.7	Differ-rence(cm)	1.8	Diffe-rence(cm)	1.875	Diffe-rence(cm)
89.1.11. (cm)	107	−3.3	107.8	−3.5	107.6	−3.6	108.2	−2.9	107.7	−1.4	107.5	+0.2	107.4	+1.8	106.7	+2.1	106.4	+1.1	104.8	+0.8
89.3.3. (cm)	110.3	−0.4	111.3	−0.1	111.2	+0.2	111.1	+1.3	109.1	+0.6	107.3	+1.1	105.6	+1.2	104.6	+1.4	105.3	+1.7	104.	+1.2
89.12.28. (cm)	110.7	+0.4	111.4	−0.5	111.0	−0.1	109.8	−0.4	108.5	0	106.2	0	104.4	−0.1	103.2	−0.1	103.6	−0.3	102.8	+0.1
90.1.27. (cm)	110.3	−0.4	111.9	−0.4	111.1	−0.4	110.2	−0.6	108.5	−0.2	106.2	−0.2	104.5	+0.3	103.3	+0.2	103.9	+0.3	102.9	−0.1
90. 2.25. (cm)	111.7		112.3		111.5		110.8		108.7		106.4		104.2		103.1		103.6		102.8	
Mean settle orlift(cm)	−0.93	Settle	−1.12	Settle	−0.98	Settle	−0.65	Settle	−0.25	Settle	+0.28	Lift	+0.8	Lift	+0.9	Lift	+0.7	Lift	+0.5	Lift

(B)

Buried depth of surveying tube (m)	0.3	Differe-nce(cm)	0.7	Differe-nce(cm)	0.9	Differen-ce(cm)	1.1	Differen-ce(cm)	1.3	Differen-ce(cm)
Surveying tube highness(cm) on Nov 1st, 1989	137	+30.3	125.6	−1.2	110.2	+1.1	95.4	+0.8	83	+3.3
Surveying tube highness(cm) on Mar. 3rd, 1989	106.7	−30.7	126.8	+0.9	109.1	+2.1	94.6	+2.3	79.7	+0.7
Surveying tube highness(cm) on Dec. 29th, 1989	137.4	−0.7	125.9	+1.8	107.0	+1.0	92.3	+1.7	79.0	+1.6
Surveying tube highness(cm) on Jan. 23rd 1989	136.7	0	124.1	−2.2	106.0	+0.8	90.6	+0.9	77.4	+0.7
Surveying tube highness(cm) on Feb. 25th, 1989	136.7		126.3		105.2		89.7		76.7	
Mean settle or lift(cm)	−0.28	Settle	−0.18	Settle	+1.25	Lift	+1.43	Lift	+1.57	Lift

large difference of the electric resistivity exists between Astrofix Hill top and the southern highland near Yan'ou Lake (the surveying lines No. 5 and No. 6 are shown in Fig 1). Although the distance between them is only 300 m, the electric resistivity on the southern highland is one magni tude higher than that on the Astrofix Hill top (Table 2).

From the analysis of the samples collected we found that, excluding the factor of the elevation (the former is 24.2 m, and the later is 41 m), the salt content produces a higher resistivity of the surface sediments.

For instance, after shaking the sediment samples with water versus soil ratio of 5:1 collected at 60—70 cm depth in the two places, we used Hitachi 180—80 atomic absorption sp-

Table 2. Resistivities of several geological bodies on Fildes Peninsula.

Name	ρ change range(Ωm)	Rock name	Water content(%)		ρ change range(Ωm)
			Sea water	Freshwater	
Sea water	$3.2\times10^{-1}\sim2.6\times10^{0}$	Basalt	0	0	$3\times10^{2}\sim8\times10^{2}$
Sediments on beach	$8\times10^{2}\sim1.2\times10^{3}$		5~10	0	$2.5\times10^{0}\sim3.7\times10^{0}$
Yan'ou Lake highland Sediment	$5.1\times10^{2}\sim9.7\times10^{3}$	Volcanic agglomerate	0	0	$3.2\times10^{2}\sim1.2\times10^{3}$
Astrofix Hill-top Sediment	$2.9\times10^{1}\sim7\times10^{2}$		5~10	0	$2.2\times10^{0}\sim3.5\times10^{0}$
Accumulating snow	$\sim10^{0}$	Volcanic breccia	0	0	$2.9\times10^{2}\sim9.3\times10^{2}$
			5~10	0	$3\times10^{0}\sim4.9\times10^{0}$

ectrograph to determine K^+,Na^+,Ca^{++},Mg^{++} contents in the solution. For determining K^+, Na^+, we added Cs to avoid ionization. For determining Ca^{++}, Mg^{++}, we added Sr to prevent disturbance of ionization. The determination result is listed in Table 3. we can see in the table that the

Table 3. Salt content of sediments underground 60— 70cm on Astrofix Hilltop and southern hill top beside Yanou Lake.

Sampling position and depth	Element content(mg/100g soil)								
	K^+	Na^+	Ca^{+2}	Mg^{+2}	CO_3^{-2}	HCO_3^-	Cl^-	SO_4^{-2}	Total salt content
Astrofix Hilltop (underground 60—70cm)	0.64	0.063	0.086	0.018	—	0.048	0.019	Untestsd out	0.874
Center of stone circle (underground 60—70cm)	0.40	0.092	0.030	0.011	—	0.048	0.019	Untested out(tiny minority)	0.60

Note: Ionic conductivity of K^+, Na^+, Ca^{+2} and Mg^{+2} is 0.143, 0.218, 0.218 and 0.224 respectively.

sediments on Astrofix Hill top contain much more major salt components, K^+ Ca^{++}, Mg^{++}, and its total salt content is 0.274mg/100g soil higher than that on southern highland near Yan'ou Lake. It is just the cause for increasing electric conductivity and reducing of electric resistivity at the surveying site. The analysis result of total salt content also indicates that the electrical conductivity of the surface sediments has a positive correlation with amount of cations, Meantime, it is directly proportional to the total salt content. On the other hand, CO_3^{-2} can not be strictly seperated from HCO_3^-, because the HCO_3^- can be dissolved into CO_3^{-2} in the weathering process of the soil, but it also absorbs the CO_2 from air turns CO_3^{-2} into HCO_3^- in the hydrolytic process. Therefore, they are always transformed into each other. The following two factors were probably responsible for the high salt content in the sediments on Astrofix Hill top. Firstly, there was a long time of transgression and the regression took place not long before present (it may explain in one aspect that the AstrofixHill top raised above sea level later than the southern highland near Yan'ou Lake), the Astrofix Hill top has been exposed to a longer oceanic effect and, therefore, larger salt was accumulated. Secondly, the wind direction may play a role. The sea-water vapor was carried by wind into the atmosphere, and then its salt component fall into the ground surface after its condensation. This process has been proved by Bian Lingen (1988), Li Hong-zhen and Lu Weixiu *et al.* (1988). Gras *et al.* (1985) have also found the similar phenomenon in the coastal region of Antarctica.

The high salt content in the active layer causes specially low electrical resistivity in the permafrost (e.g. the electrical resistivity of permafrost is above 1000 Ωm in TianShan region, China, Cui Zhijiu & Zhu Cheng (1988), but the electrical resistivity of the permafrost can be as low as $10^2\Omega$m on Fildes Peninsula which is exposed to sea water). The exsistence of a thicker unfrozen layer of a part of sediments under the cold subpolar climate results in formation of active layer in this region which is fully defferent from that in the intracontinental region of the northern hemisphere. It is the high salt content which has transformed the frost state of the active layer and made the frost intensity and depth in this region much less than that in the alpine periglacial area of continental climate. Therefore, in unfrost state, striated soil which is a typical periglacial landform creeping on the surface becomes a mostly developed and widespread landform in this region. Furthermore, the exsistence of the permafrost table makes the salt in surface sediments no easier to percolate into the lower frozen layer, the high salt content makes the freezing point of the permafrost reduce and the permafrost no easier to freeze and heave. Thus, the result of measurement with layering frost heaving instrument shows a general tendency of "settlement of upper part and up lifting of lower part", except in winter and hard observational seasons. It is just contrary to our observation in the Tianshan periglacial region of China (Cui Zhijiu, & Zhu Cheng, 1991.) In the area studied, the salt content is also important for periglacial landform development. On the southern highland where salt content is lower, one can find widespread sorted circles, sorted strips and net, as well as stone flowers. But the Astrofix Hill top where salt content is much higher, few periglacial landforms can be found. It reflects a control effect of salt content on the development of periglacial landforms.

4. Electrical resistivity sounding of subsurface part below the active layer

After the pitting and measuring electrical parameters, we used DDC-2A electron automatic compensator with Schlumberger's symmetric 4 probes method for electrical resistivity sounding many times. The sounding sites are shown in Fig. 1.

The structural features of subsurface land-sea-ice-bedrock in the area can be explained from the original curve of the electrical resistivity sounding in Fig. 8.

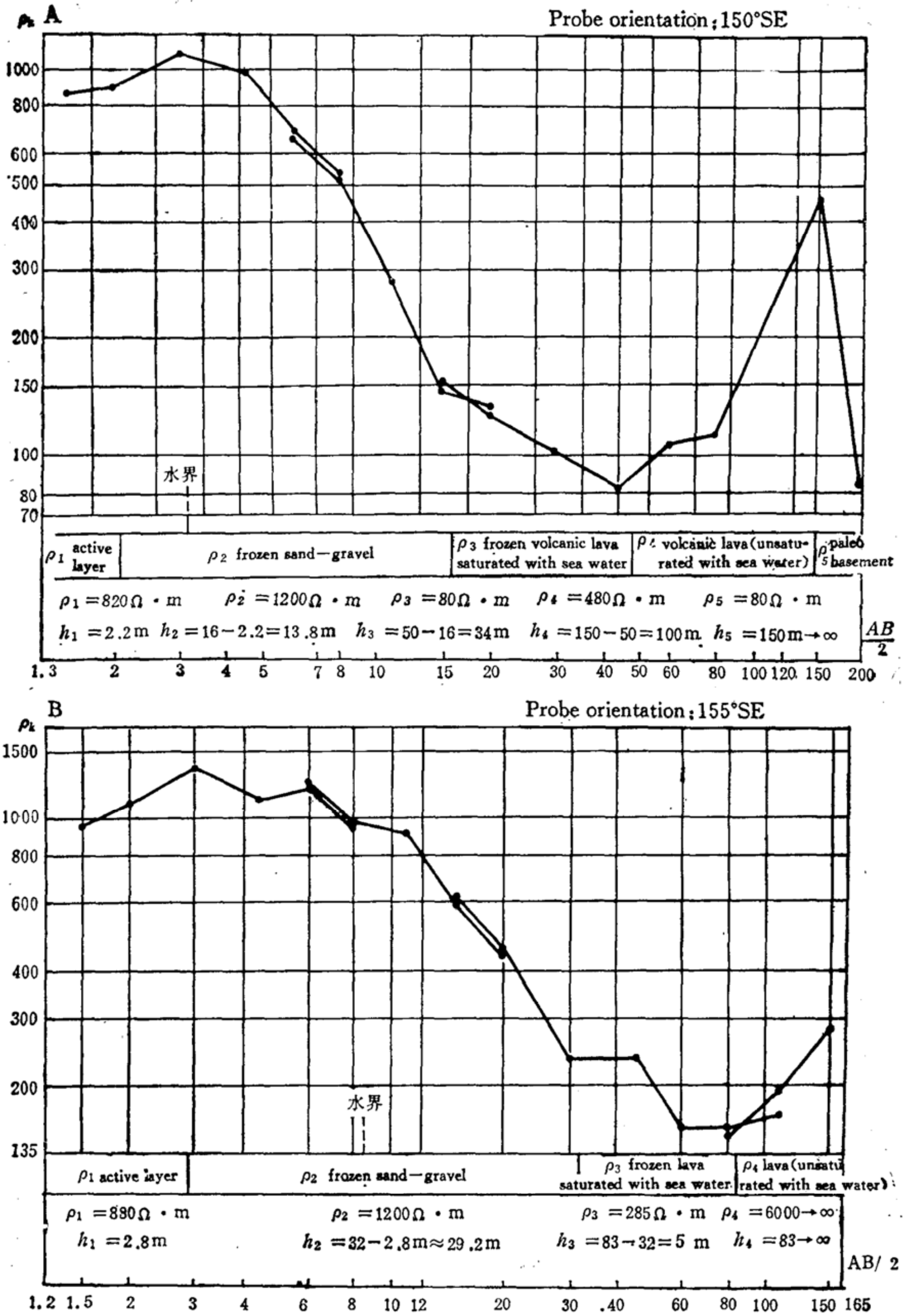

Fig. 8. Original curve No. 3 (A) and No. 4 (B) of the geoelectrical prospectings on Fildes Peninsula.

The profile of curve No. 3 lies on the beach terrace at elevation of 3 m and 40 m from the coast (see Fig. 1) and profile of curve No. 4 is parallel to it, but 200 m from the coast and at elevation of 5 m higher than the former. We found that both the two curves belong to KHK type curve (i.e. $p_1<p_2>p_3<p_4>p_5$). The original curve No. 3 shows that the structure, in the area can be divided into five layers. The first layer is active layer with electrical resistivity of 820 Ωm and thickness of 2.2 m (determined after pitting and threelayer graticule); the second layer represents frozen beach sand-gravels after pitting and in-situ observation. Because the level of 3.2 m depth is identical with the average sea level, the electrical resistivity from 3.2 m to 16 m depth sharply decreases from 1200 Ω m with increasing salinity of underground sea water. The resistivity curve of the frozen layer is very different from K-type curve (that is $p_1<p_2>p_3$) obtained in permafrost region of china. In recent years, this frost phenomenon existing under the sea level in the Antarctic region has been proved to be also in the "offshore subsea permafrost" (Washburn, 1980) in the process of oil and gas exploration along the Arctic coast of Alaska.

The third layer is frozen volcanic lava (mainly basalt) with the electrical resistivity of 80Ωm, at depth of 16–50 Ωm. The conclusion is reached on the basis of observation on the exposed bed rock and the electric-parameter testing conducted after bed rock is saturated with sea water. Table 2 shows that the electrical resistivity of the sea water can be as low as 3.2×10^{-1} Ωm, while for the basalt containing 5—10% sea water, its ρ value can reduce to two order of magnitude as compared with that uncontaining sea water. Then, why the electrical resistivity of 80–140Ωm on the curve No. 3 is produced by volcanic rock (basalt)? We considered that it is determined by the property of the frozen rock body. From the electrical conductivity, when unfilled with sea water, the pores of the porous volcanic massive only plays a role of insulation and increasing resistivity. But after filling with sea water, Na^+,Cl^- and other conductive ions in the water can increase the conductivity of the rock body and reduce the electrical resistivity. At that time, the rock body just likes numerous small resistances in series (Fig. 9.)

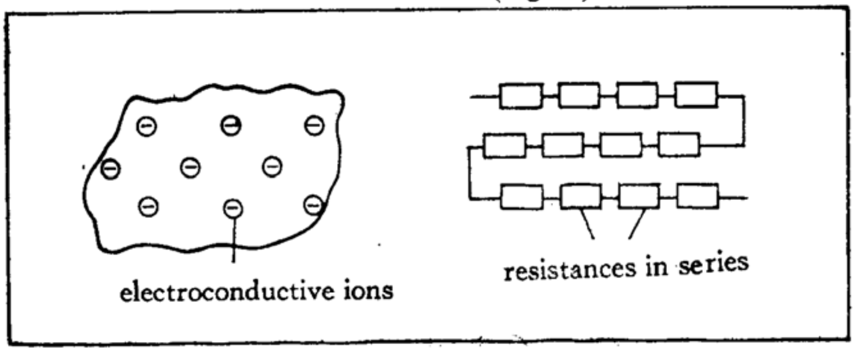

Fig. 9. Distribution of the electroconductive ions of the porous volcanic rock filled with sea water (left) and resistances in series (right).

But when the rock body is frozen, the ice has a high electrical resistivity (it can reach to $10^5\Omega$ m), and the ions in the ice can not migrate since the water solution is in frost state, therefore, the electrical resistivity of the rock body also increases. At depth of 50–150m beneath the sounding site No. 3 should be the frozen volcanic rock which is free from the influence of the sea water. Because the layer structure is compact (the heavy load of its covering layer makes its porosity decrease) and sea water can not be easily percolated, its electrical resistivity can increase up to 480 Ωm in frost state. But at 150 m depth, the curve of the electrical resistivity shows a sudden change, which, we think, shows an interface results from the thawing by upper layer load and increasing geotherm. Since the lower bed rock is essentially different from the upper volcanic rock in terms of thermophysical and chemical properties, the layer below 150 m depth should be considered to be older and deeper metamorphic "Pre-Jurassic basement" (Liu Xiaohan & Zheng Xiangshen, 1988).

The topographical condition led to arrange electrodes spacing of 300 m on the sounding site No. 4. Its original curve (Fig.8) shows that heve the active layer is 2.8m thick(calculated with three-layer graticule), frozen sand-gravel is 29.2 m thick, the depth of sea water interface is 8m. The frozen bed rock influenced by sea water is about 51 m thick. At 83 m depth, the asymptote of the electrical resistivity is at an angle of 45° with the horizontal axis, it satisfies the formula $\lg\rho_S = \lg\frac{AB}{2} - \lg s_1$ (Changchun Geology College, 1980). In the formula, $s_1=\frac{h_3}{\rho_3}$, it is the longitudinal conductive value of the third layer, and yet the sounding profile at MN site has an current intensity, $j_{MN}=2j^{A}_{MN}=2+\frac{I}{2\pi l\, h}=\frac{I}{\pi l\, b}$(Xi'an Geology College, 1979). The ρ_4 should be at least $> 20\times285\ \Omega m$ and $\to\infty$. But according to the topography and the sounding curve No. 3, we considered that at underground 150 m depth beneath the site would be an paleo-continental basement with a decreasing electrical resistivity.

The sounding site No. 6 is located in the south highland area near Yan'ou Lake, its average electrical resistivity is shown in Table 2. Our pitting (Fig. 3) has revealed its layering features . Because the sounding curve No. 1 and No. 2 have their similar characteristics with the curve No. 3 and No. 4, we needn't to describe repeatly.

Finally, summerizing the above-described information, combining with a correlation analysis of measured geotemperature at 0.4, 0.8, 1.6 m depths on the meteorological station of the Great Wall Station from 1985 to present, if ignoring the salt content, we can deduce a general vertical gradient of the permafrost table on the Fildes Peninsula to be 3–5 / 100 with the elevation change. In other words, when the elevation rises (or declines) 10m, the permafrost table will correspondingly rise (or decline) 0.3-0.5m based on the permafrost table at 1.5 m depth at the Astrofix Hill top.

References

Araya, R. & Herve, F., (1972): Periglacial phenomena in the South Shetland Islands, *Antarctic Geology and Geophysics*.

Bian Lingen & Jia Peng-qun (1988): Observation and Research on the Antarctic Meteorology, *Antarctic Research Chinese Edition*, Vol. 1, No. 1, 57—61.

Cui Zhi jiu & Zhu Cheng (1988): Rock glaciers in the source region of Urumqi River, Middle Tian Shan, China, Fifth International Conference on Permafrost, Proceedings Vol. 1, Trondheim, Norway, 724—727.

Changchun Geology College (1980): Hydrogeology and Engineering Geology, Geology Press, 1—169.

John, B. S. (1972): Evidence from the South Shetland Islands towards a glacial history of West Antarctica, Polar Geomorphology', Inststute of British Geographers Special Publication, 75—92.

Liu Xiao han & Zheng Xiang-shen (1988): Geology of volcanic rocks on Fildes Peninsula, King George Island, West Antarctica, *Antarctic Research*, Vol. 1, No. 1, 25—34.

Shi Ya feng, Cui Zhijiu & Li Ji jun (1989): Quaternary Glacier and Environment in East China, Science Press,35—187.

Washburn, A. L. (1980): Focus on Polar Research, *Science*, Vol. 209, P. 643.

Xi an Geology College (1979): Electric Prospecting, Geology Press, 73—75.

Xie You yu (1988): Chemical weathering in permafrost regions of Antarctica, Great Wall Station, Casey Station and Davis Station area *Antarctic Research* Vol. 1, No. 2, 8—13.

Zhang Qing song (1990), A comparison of periglacial landforms on the Vestfold Hills, east Antarctica, and on the Fildes Peninsula, West Antarctica *Antarctic Research* Chinese Edition, Vol. 2, No. 1, 1—9.

Zhu Cheng (1988), A superficial discussion of talus at the head of Urumqi River, Tian Shan, *Mountain Research*, Vol. 6, No. 4, 204—209.

Zhu Cheng (1989): The characteristics of the surface movement of the lobate-shape rock glacier from the debris fabric, Tian Shan, China, *Journal of Glaciology and Ceocryology*, Vol. 11, No. 1, 82—88.

(*received 1990*)

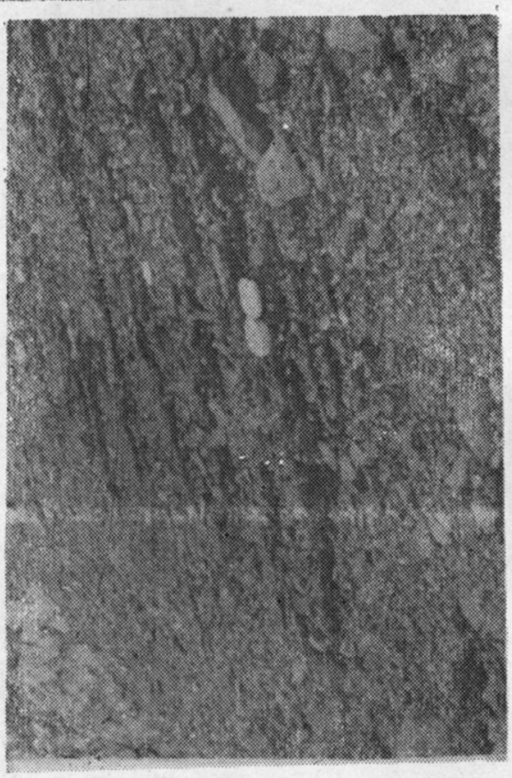

Photo 1. Striated soil on Fildes Peninsula.

Photo 2. Debris flower on southern hill top near Yanou Lake.

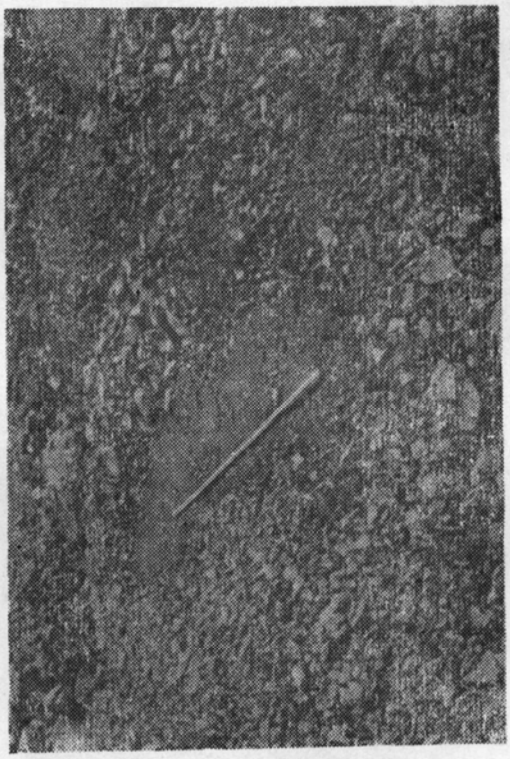

Photo 3. Sorted debris circle No. 3 on the southern hill top near Yanou Lake.

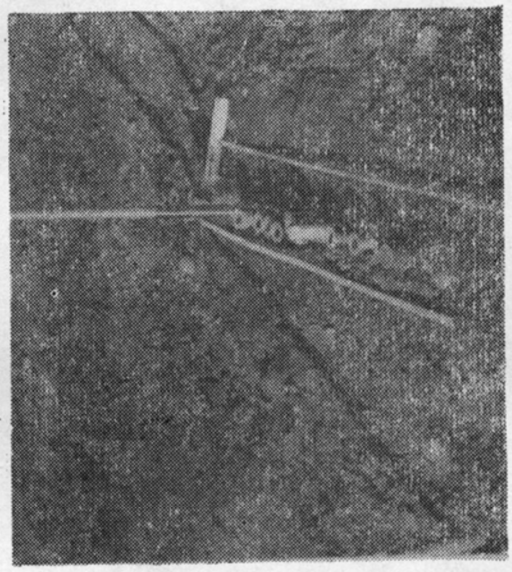

Photo 4. Layering frost-heaving instrument installed on the Astrofix Hill top.